

TURBULENT KINETIC ENERGY BUDGET ON MARS. DERIVATION FROM GROUND-BASED DATA.

G. M. Martínez, L. Vázquez, *Department of Applied Mathematics, Faculty of Informatics, Universidad Complutense de Madrid, Spain (mmgerman@fis.ucm.es), F. Valero,* *Department of Earth Physics, Astronomy, and Astrophysics II, Faculty of Physics, Universidad Complutense de Madrid, Spain.*

Introduction

We present in this abstract the first estimation of the turbulent kinetic energy (TKE) budget from ground-based data on Mars. The comparative role of advection, buoyancy, shear, turbulent transport, turbulent pressure redistribution, and dissipation has been determined during the most convective hours, both for the lowest Surface Layer (SL), and for the upper Convective Mixed Layer (CML).

This study has been carried out from ground-based data corresponding to Viking 1, Viking 2, and Pathfinder (PF) missions, and from an adaptation of similarity theory to Mars, creating a new approach to research the Martian TKE budget [1]. Specifically, the set of data consists of: (i) in situ hourly-averaged temperature, (ii) in situ hourly-averaged horizontal wind speed measured at the same height as temperature, and (iii) modeled hourly ground temperature—derived using the model presented in [2]. They all belong to 3 selected entire Martian Sols, namely: Sol 25-26 of PF; Sol 28 of Viking Lander 1 (VL1); and Sol 20 of Viking Lander 2 (VL2).

Using this simple scheme—compared to the time-costing Large Eddy Simulations (LES)—, some of our results have been found to compare well to already published LES outcomes [3, 4], which increases our confidence in our new results and methodology.

Methodology

The evolution of the TKE in the Reynolds average form, under the Boussinesq approximation, the assumption of Newtonian fluid, and Einstein notation [5], can be written as

$$\begin{aligned} \frac{\partial \bar{e}}{\partial t} = & -\bar{U}_j \frac{\partial \bar{e}}{\partial x_j} + \delta_{i3} \frac{g}{\theta} \overline{u_i \theta'} - \\ & -\overline{u_i' u_j'} \frac{\partial \bar{U}_i}{\partial x_j} - \frac{\partial \overline{u_j' e}}{\partial x_j} - \frac{1}{\bar{\rho}} \frac{\partial \overline{u_j' p'}}{\partial x_j} - \epsilon, \end{aligned} \quad (1)$$

where \bar{U}_j stands for the mean wind speed, $\bar{\rho}$ for the mean air density, ϵ for the dissipation term, and u_j' , θ' , and p' for the turbulent deviation of the velocity, potential temperature, and pressure, respectively.

Equation (1) states that TKE can vary (storage term on left side) as a consequence of different mechanisms shown on the right side. It can be advected by the

mean wind, generated or destroyed by buoyancy and shear, transported by the turbulent transport and turbulent pressure redistribution terms, and finally destroyed via molecular dissipation, respectively.

We can rewrite Equation (1) for convenience as

$$\begin{aligned} 0 = & \frac{g}{\theta} \overline{w' \theta'} - \overline{u' w'} \frac{\partial \bar{U}}{\partial z} - \frac{\partial \overline{w' e}}{\partial z} - \epsilon + R = \\ = & Bu + Sh + Tr - Diss + R, \end{aligned} \quad (2)$$

where Bu stands for buoyancy, Sh for the main shear term, Tr for the vertical turbulent transport, $Diss$ for dissipation, and R for the “residual” term, which involves the storage term, the advective term, the pressure redistribution term, two terms accounting for the horizontal turbulent transport of TKE, and finally, eight terms accounting for the shear, as can be deduced from Eqs. (1) and (2).

From the mentioned ground-based data, and via an adaptation to Mars of similarity theory, we have obtained values for each of the terms involved in Eq. (2), both for the SL and the CML [1, 6]. The term R has been calculated precisely as the residual ($R = -Bu - Sh - Tr + Diss$) of this equation and is expected to be small, having a low contribution to the TKE budget.

Results

Surface Layer TKE Budget

The SL TKE budget for PF Sol 25 is shown in Figure 1. Shear is the main source of TKE, which is expected at heights close to the ground. On the contrary, dissipation becomes the main sink of TKE, barely exceeding the shear production. Both mechanisms present values on the order of $10^{-1} \text{ m}^2 \text{ s}^{-3}$. Buoyancy and the vertical turbulent transport balance each other, and are one order of magnitude lower than shear and dissipation. Specifically, buoyancy is positive (generation of TKE) since the surface kinematic heat flux was directed upwards close to noon. The vertical turbulent transport is negative instead, which indicates that it is removing TKE from the SL by sending it upwards. Finally, the residual term, though higher than the minor buoyancy and transport terms, is still about 30% of the ruling shear and dissipation mechanisms. It can be likely attributed to the advective term, to the horizontal shear, and to the

TKE Budget

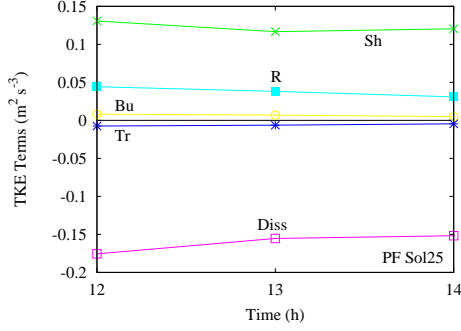


Figure 1: TKE budget in the Surface Layer for PF Sol 25. Estimated at 1.3 m. The results span the most convective hours (from 1200 h to 1400 h, local solar time), when the TKE is expected to be steady. *Bu*, *Sh*, *Tr*, *Diss*, and *R* stand for buoyancy, shear, vertical turbulent transport, dissipation, and the residual term, respectively. See Eq. (2) for their definitions.

pressure redistribution term. The storage and horizontal turbulent transport terms unlikely account for the found imbalance.

The SL TKE budget for VL1 Sol 28 is shown in Figure 2. Despite corresponding to two different Mar-

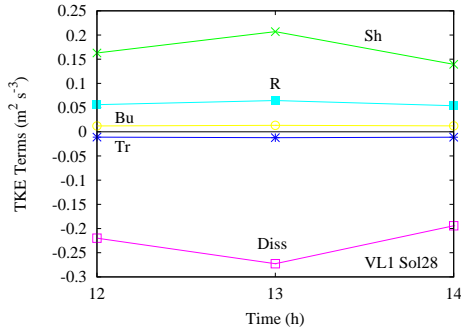


Figure 2: As Figure 1, but for VL1 Sol 28 estimated at 1.6 m.

tian locations, the results for PF Sol 25 and VL1 Sol 28 present striking similar features. This fact gives consistency to the results in the sense that, provided that the meteorological conditions are similar—as it was the case for both landing sites during each first summer—the SL TKE budget for any mid latitude northern summertime Sol under no baroclinic disturbances and over moderately flat terrains should not differ notably from the ones presented in Figures 1 and 2.

The synoptic conditions during VL2 Sol 20 were not as steady as for PF Sol 25 and VL1 Sol 28; the atmospheric distortion was higher during the VL2 first summer, and so was the dust content. This fact implies that the SL TKE budget for the VL2 Sol 20, shown in Figure 3, presents an anomalous behaviour. Shear is no longer the main TKE generator, and shows values around

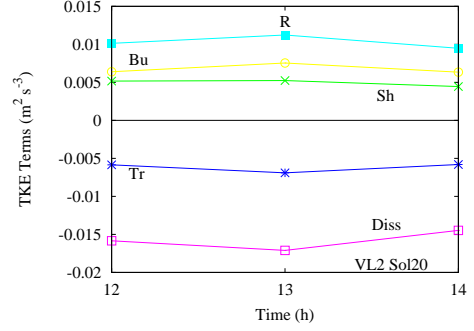


Figure 3: As Figure 1, but for VL2 Sol 20 estimated at 1.6 m.

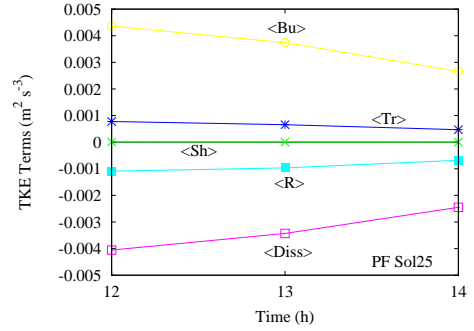


Figure 4: TKE budget in the Convective Mixed Layer for PF Sol 25. The brackets indicate average in the range $0.2z_i-0.8z_i$ (with z_i the PBL height), through which the turbulent heating dominates the radiative one, and thus the methodology is more accurate. $\langle Bu \rangle$, $\langle Sh \rangle$, $\langle Tr \rangle$, $\langle Diss \rangle$, and $\langle R \rangle$ stand for the vertically averaged buoyancy, shear, vertical turbulent transport, dissipation, and the residual term, respectively.

$5 \times 10^{-3} \text{ m}^2 \text{ s}^{-3}$. Buoyancy is slightly higher than shear, and also contributes to the generation of TKE. Dissipation is the principal TKE remover, with values $\sim 10^{-2} \text{ m}^2 \text{ s}^{-3}$, which exceeds by one order of magnitude the shear and buoyancy productions. The vertical turbulent transport removes TKE at the same rate than buoyancy generates it. But the most striking feature is the high value of the residual term, which becomes the main generator of TKE. Thus, any of the terms accounting for *R*, which were included in the residual term due to their pre-supposed minor role, becomes now relevant. Advection and shear (excluded the “principal” shear term $\overline{u'w'} \frac{\partial \overline{U}}{\partial z}$) are very likely to account for it, while the storage and horizontal turbulent transport terms are not. Finally, little can be said about the pressure redistribution term, which is beyond the scope of this study.

Convective Mixed Layer TKE Budget

We turn to the CML, and show its TKE budget for PF Sol 25 and VL1 Sol 28 in Figures 4 and 5, respectively.

TKE Budget

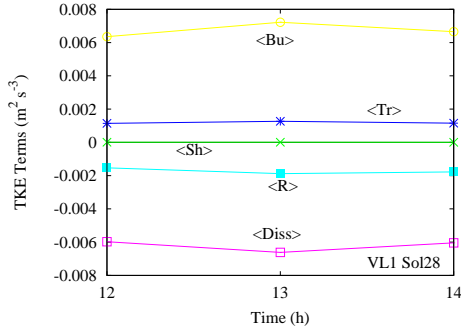


Figure 5: As Figure 4, but for the VL1 Sol28.

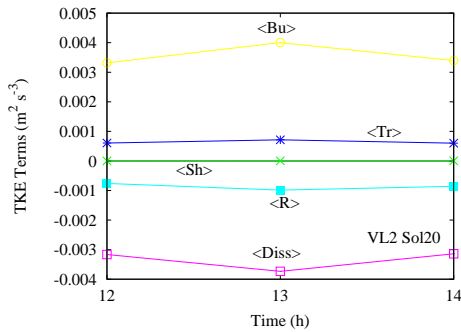


Figure 6: As Figure 4, but for the VL2 Sol20.

Buoyancy becomes the principal source of TKE, presenting values around $5 \times 10^{-3} \text{ m}^2 \text{ s}^{-3}$. On the other hand, shear can be considered negligible ($\sim 10^{-6} \text{ m}^2 \text{ s}^{-3}$), since convection tends to homogenize the vertical profile of the horizontal wind. Dissipation balances buoyancy, thus being the main mechanism removing TKE. The vertical turbulent transport term plays a minor role compared to the dominant mechanisms, with values $\sim 10^{-4} \text{ m}^2 \text{ s}^{-3}$. Unlike in the SL, it is positive, and therefore, on average, the CML is receiving TKE from the SL, from where TKE is exported upwards. Fi-

nally, the imbalance, which is negative and almost equal in magnitude to the vertical turbulent transport term, represents around 25% of buoyancy or dissipation (main mechanisms). It can be likely attributed to the advective and horizontal shear terms. The pressure redistribution term cannot be neglected either, since very little is known about it.

With regard to the CML TKE budget for VL2 Sol 20, we believe that the methodology employed “forces” the results to look like those obtained for PF Sol 25 and VL1 Sol 28, as can be seen in Figure 6. During these two Sols, unlike through VL2 Sol 20, there were both low radiative heating compared to the turbulent one across the CML (low dust content), and no baroclinic disturbances. Thus, the methodology employed is expected to be more accurate.

References

- [1] Martínez GM, Valero F, Vázquez L. 2010. TKE Budget in the Convective Martian PBL. Submitted to *Q. J. R. Meteorol. Soc.*
- [2] Savijärvi H, Määttännen A, Kauhanen J, Harri AM. 2004. Mars Pathfinder: new data and new model simulations. *Q. J. R. Meteorol. Soc.* **130**: 669-683.
- [3] Spiga A, Forget F, Lewis S, Hinson D. 2010. Structure and dynamics of the convective boundary layer on Mars as inferred from large-eddy simulations and remote-sensing measurements. *Q. J. R. Meteorol. Soc.* **136**: 414-428.
- [4] Michaels TI, Rafkin SCR. 2002. Large-eddy simulation of atmospheric convection on Mars. *Q. J. R. Meteorol. Soc.* **130**: 1251-1274.
- [5] Stull R. 1988. *An Introduction to Boundary Layer Meteorology*. Springer.
- [6] Martínez GM, Valero F, Vázquez L. 2009. Characterization of the Martian Convective Boundary Layer. *Journal of the Atmospheric Sciences* **66**: 2044-2058.